SPECULAR RADAR SCATTERING FROM BURIED CRATER EJECTA. Thomas W. Thompson and Eugene A. Ustinov, Jet Propulsion Laboratory, California Institute of Technology, 4800 Oak Grove Drive, Pasadena, CA 91109, USA: twthompson@jpl.nasa.gov, phone: 818-354-3881, fax: 818-393-5285

Context: - This is an update to our previous investigation of radar scattering from buried crater ejecta that was described in Thompson et al. (2011) [1]. As shown in Figure 1, we assume that lunar radar scattering can be associated with three scattering mechanisms (specular scattering from the space–regolith interface, specular scattering from buried layers, and diffuse scattering from wavelength-sized surface and sub-surface rocks). Specular scattering from the surface–space interface is characterized by echoes, which are only in the opposite sense circular (OC) component and have a strong dependence on angle of incidence that is proportional to $\cos^{1.5}(\Theta)$. Diffuse scattering from surface and subsurface rocks is characterized by echoes, which have same-sense circular (SC) and OC components with a dependence on angle of incidence proportional to $\cos(\Theta)$.

Modeling Assumptions: Here, we assume that regolith density differences associated with the buried crater ejecta layers seen in the Apollo core tubes can be modeled by a single sub-surface layer with a greater dielectric constant. With refraction through the space–regolith interface accounted for, specular scattering from this single buried layer produces OC echoes that dominate average lunar radar echoes with angles of incidence from about 20° out to about 80°degrees.

This modeling also produced results consistent with the data obtained by Hagfors et al. (1965) [2] where the Moon was illuminated from Earth by radar with circular polarization and echoes were recorded in orthogonal linear polarizations as shown in Figure 2. As seen on the left panel of the Figure 2, ranging in delay localizes echoes to a ring that is centered on the sub-radar point as seen from earth. Spectral analysis of echoes from this ring separates echoes into strips that are parallel to an apparent axis of rotation (the libration axis in Figure 2). Scattering areas vary across the range ring, so that minimum reflecting areas occur where the range ring intersects the libration axis of the Moon. The largest reflecting areas occur for those furthest from the libration axis.

The results of this experiment (right panel of Figure 2) indicate that there is a difference in the echo powers in the orthogonal linear polarizations.

Modeling Results: A quantitative description of radar scattering from a single buried specular-scattering layer was formulated in Appendix C of (Thompson et al., 2011) [1]. It was shown there that the modeled angular dependence of total backscatter from this buried layer agrees well with the average scattering from the lunar surface as described by Hagfors (1970) [3]. Also, when refraction through the space–regolith interface was accounted for and a dielectric constant of 2.0 was assumed for the less-dense upper regolith layer, the modeling produced differences in linear polarizations that are consistent with the results shown in the right panel of Figure 2.

A re-examination of this modeling produced results consistent with the Hagfors' observations for a dielectric constant of 2.4 for the less-dense upper regolith layer. The accepted dielectric constant for the Moon at centimeter wavelengths is 2.7. A mixture of 95% dust with dielectric constant of 2.4 and 5% rocks with dielectric constant of 9.0, produces a dielectric constant of 2.7 - the accepted value for the Moon's dielectric constant).

Summary: Modeling of radar backscattering from buried crater ejecta seen in the Apollo core tubes by a less-dense upper regolith overlaying a specular-scattering layer produces results consistent with the lunar radar experiment conducted by Hagfors in the 1960's. This modeling also provides an explanation of why average lunar echoes have a $\cos^{1.5}(\Theta)$ dependence for angles of incidence from about 20° to about 80° degrees.

References: [1] Thompson, T. W., et al. (2011), *J. Geophys. Res. 116*. [2] Hagfors, T. et al. (1965), *Science, 150*, 1153–1156. [3] Hagfors, T. (1970), *Radio Science, 5*, 189–227.

.

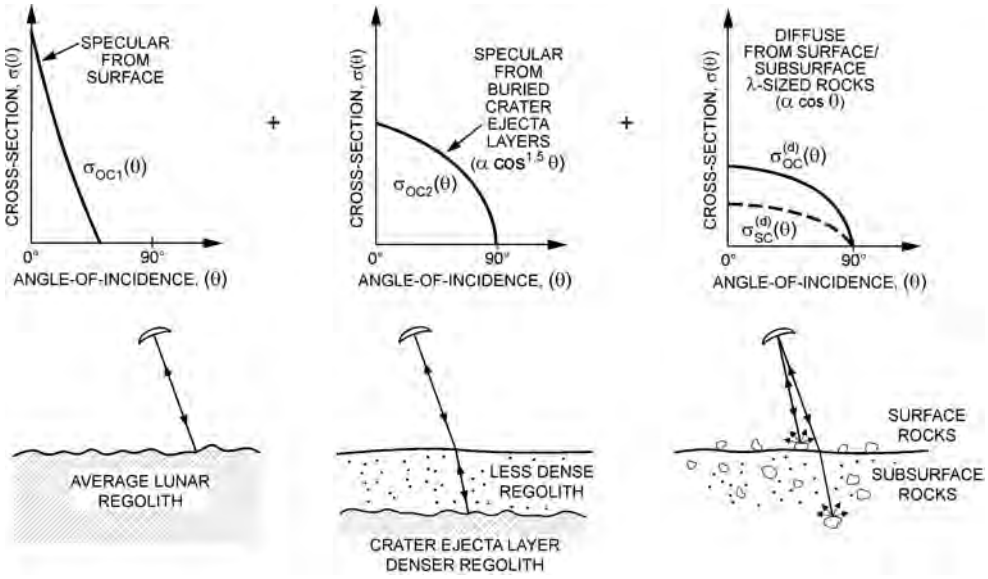

Figure 1. Specular and diffuse components of lunar radar backscatter and associated lunar surface conditions. Specular scattering from a buried crater ejecta layer is modeled by a single, denser regolith layer beneath a less-dense regolith layer.

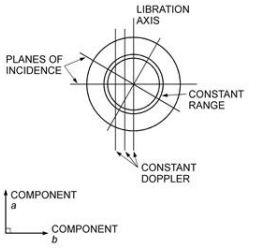

Figure 1. Schematic view of the lunar disk with range-doppler coordinates and with the two received linearly polarized components *a* and *b*

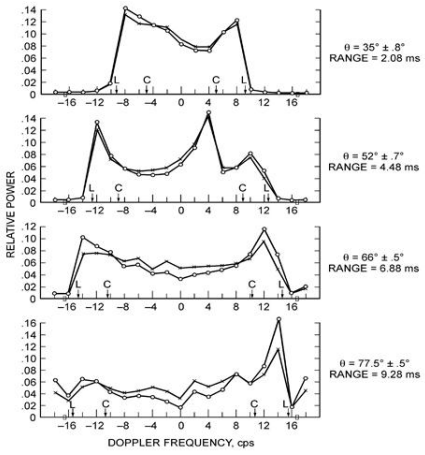

Figure 2. Normalized frequency spectra of the moon, 18 June 1965, 0340 to 0435 E.S.T., for four range rings. Ranges in milliseconds (ms): λ, 23 cm; pulse length, 200 μsec; frequency box, 2 cy/sec. *L*, maximum frequency; *C*, crossover point. Curves: –x–, E-field aligned with libration axis; –o–, *E*-field normal to libration axis.

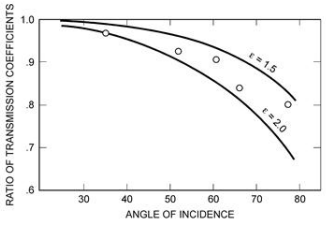

Figure 3. Ratio of transmission coefficients derived from data as compared with theoretical predictions

Figure 2. Overview of Hagfors' lunar radar experiment (Hagfors et al., 1965) [2]. Left panel shows experimental geometry; center panel shows raw results; and right panel shows results in terms of the transmission coefficients versus angle-of-incidence. Our new modeling produces good fits to the data in the right panel for a dielectric constant of 2.4 for the less dense regolith shown in the center panel of Figure 1.

Acknowledgement: This work was carried out at the Jet Propulsion Laboratory, California Institute of Technology, under a contract with the National Aeronautics and Space Administration.